On the dynamic growth of a 180° domain in a ferroelectric material

Biao Wang and Zhongmin Xiao

Citation: Journal of Applied Physics **88**, 1464 (2000); doi: 10.1063/1.373840
View online: http://dx.doi.org/10.1063/1.373840
View Table of Contents: http://aip.scitation.org/toc/jap/88/3
Published by the American Institute of Physics

On the dynamic growth of a 180° domain in a ferroelectric material

Biao Wang[a] and Zhongmin Xiao
School of Mechanical and Production Engineering, Nanyang Technological University, Singapore 639798, Singapore

(Received 4 November 1999; accepted for publication 3 May 2000)

This article investigates the dynamic movement process of a 180° domain wall in an external electric field. By modeling the domain wall movement as a dynamic process, the induced electric and magnetic fields due to a growing general ellipsoidal 180° domain under the action of a given electric field was derived explicitly. A general form of the energy release rate was derived through a surface integral, which can serve as the driving force for the movement of the surface. Based on the solution, the released electromagnetic energy during the dynamic process was evaluated. This electromagnetic energy is used to compensate the surface energy increase and the energy dissipation due to the finite velocity of the domain wall movement. Following the result, an equation is established to determine the growth speed of the 180° domain. Finally, the cases where the domain shape is cylindrical and spherical, and the domain wall propagates along the radial direction and the applied electric field direction, respectively, were considered in detail as illustrative examples. It is found that the resistance caused by the depolarization field for the wall to grow along the direction of the applied electric field is only one fifth of the value for the wall to grow along the radial direction. © *2000 American Institute of Physics.* [S0021-8979(00)07615-5]

I. INTRODUCTION

Ferroelectric crystals have been increasingly used in actuator designs for various engineering applications. The commonly used ferroelectric materials in actuator applications are polycrystalline oxide ceramics of barium titanate ($BaTiO_3$) and ($Pb[Zr,Ti]O_3$) (PZT). Barium titanate and PZT both have the perovskite cubic structure in the paraelectric phase. At room temperature, barium titanate has a tetragonal structure, while PZT has a tetragonal structure on the Ti-rich side and has a rhombohedral structure on the Zr-rich side, except that on the extreme Zr-rich side the solid solution exhibits no observable ferroelectric effect. The commonly used PZT is on the Ti-rich side near its morphotropic phase boundary because of the strong electromechanical coupling effect. The tetragonal structure is in a polar state in the sense that the centers of positive and negative charges for each lattice unit are spatially separated, forming a dipole of electric charges. Consequently, these crystals exhibit spontaneous polarization. In the stable configuration, each crystallite is divided into a number of macroscopic regions in which the polar directions differ from each other. These regions are called the ferroelectric domain. The commercial barium titanate and PZT ceramics are produced from polycrystalline solid solutions through the conventional steps of sintering fine powders of oxide metals into solutions. The resulting solid solutions do not exhibit the observable electromechanical coupling effect because the ferroelectric domains are formed in random directions so that the average polarization of each grain is approximately zero. The ceramics exhibit the electromechanical coupling effect only after the domains are reoriented by application of a strong dc field. This reorientation process is the so-called poling process. Ferroelectric domains are initially formed when the ceramics are cooled from high processing temperatures and they are altered during the subsequent poling process, leading to a macroscopic polarization. A load can switch the polar direction from one to another. An electric field may switch the polar direction by either 180° or 90°, but a stress loading may only switch it by 90°. Also it is a well-known fact that the crystal changes its state progressively by domain wall movement under the action of external field, and the domain wall movements underlie all phenomena of polarization and deformation. Since they have profound effects on the functions of devices made of ferroelectrics, a lot of research has been done to understand the phenomena related to the domain switch. In an early study, Landauer[1] considered the possible formation of thermally induced, spike-shaped domains of reversed polarization in $BaTiO_3$. Rickman *et al.*[2] presented a treatment of twin domain formation energetics in ferroelectric materials. Speck *et al.*[3] described domain formation in epitaxial systems in terms of a defect theory. The kinetics of domain wall evolution were considered by Loge and Suo.[4] Gopalan and Mitchell[5] carried out a systematic study of the switching time, domain wall velocities, and stabilization mechanisms of 180° domains in *Z*-cut $LiTaO_3$ crystals. Huo and Jiang[6,7] and Rosakis and Jiang[8] proposed a continuum model for domain switching in polycrystalline ferroelectric ceramics, and studied the morphology of ferroelectric domains. Lynch and McMeeking[22] and Hwang *et al.*[9] examined the nonlinear behavior of PLZT based on a domain switching mechanism. Lu *et al.*[10] also investigated the nonlinear electromechanical behavior related to ferroelectric and ferroelastic domain switching. Yang and Suo[11] studied the cracking phenomenon in ceramic actuators related to the domain switching process. Li

[a]Author to whom correspondence should be addressed; on leave from Harbin Institute of Technology, Harbin, China; electronic mail: mwangb@ntu.edu.sg

and Weng[12] developed a micromechanical theory for the nonlinear behavior of ferroelectrics. Yang *et al.*[23] made a direct optical observation of pinning and bowing of a single 180° ferroelectric domain wall under a uniform applied electric field using a collection mode near-field scanning optical microscope. Chai *et al.*[24] proposed a domain model for ferroelectric films. However, all the aforementioned analyses assumed that the domain switching process was quasistatic. As a result, the energy related to the domain switching was obtained by modeling the procedure as an electrostatic problem. In fact, the domain wall is observed to move at a wide range of velocity (10^{-9}–10^{-1} m/s), and the higher the applied electric field and temperature, the faster the wall moves. Therefore, as referred by Loge and Suo,[4] domain evolution is a nonequilibrium dynamic process. As the domain grows in a certain speed, it cannot only create a depolarization electric field, but also create a magnetic field around the domain. Thus part of the released energy in the process of domain wall movement is used to create the magnetic field in addition to complementing the surface energy increase.

In this article, a 180° domain is considered to be initiated inside a parent ferroelectric domain, and the 180° domain wall grows in some unknown speed under the action of the electric field opposite to the polar direction of the ferroelectric material. Due to the growth of the 180° domain wall, a magnetic field is induced surrounding the domain. The internal and external electric and magnetic fields for an ellipsoidal domain are derived through solving the dynamic problem. Through studying the movement of the 180° domain wall in an electromagnetic field, a general form of the energy release rate was derived through a surface integral. As the energy release rate serves as the driving force for the movement of the surface, an equation for determining the growth speed of the 180° domain wall is derived. As illustrative examples, a cylindrical and a spherical domain were considered in detail. For the spherical 180° domain, it is found that the minimum electric field needed for the wall to propagate along the direction of the applied field is only one fifth of the value needed for the wall to propagate along the radial direction.

In order to have a more clear and practical picture of the various points emphasized in this article, a typical ferroelectric material, barium titanate, is used for detailed numerical calculation. $BaTiO_3$ undergoes a phase transition at a temperature of about 130 °C. Above 130 °C, the crystal is cubic, and the ions lie symmetrically in the unit cell. Between 0 and 130 °C, the crystal is tetragonal, and the ions lie asymmetrically in the unit cell. A tetragonal unit cell may have polar direction of any six variants. A load can rotate the polar axis from one direction to another. We will use barium titanate to illustrate the various points in this article.

II. THE PHYSICAL PROBLEM AND FORMULATION

Consider the physical problem where a parent ferroelectric crystal contains a 180° ellipsoidal domain under the action of a uniaxial electric field $\vec{E}_0$ along the z axis as shown in Fig. 1(a). The 180° domain grows in some unknown speed. Since the spontaneous polarization plays a role as the external field source, to obtain the induced electric and magnetic fields by an ellipsoidal growing 180° domain, we can decompose the original problem shown in Fig. 1(a) into the following two subproblems: (1) under the action of the applied electric field, a ferroelectric crystal with spontaneous polarization $\vec{P}_S$ along the opposite direction of the electric field [Fig. 1(b)]; (2) in the dielectric medium there is a growing 180° domain with polarization $2\vec{P}_S$ along the direction of the applied electric field [Fig. 1(c)]. The superposition of the two solutions gives the solution of the original problem for a linear medium.

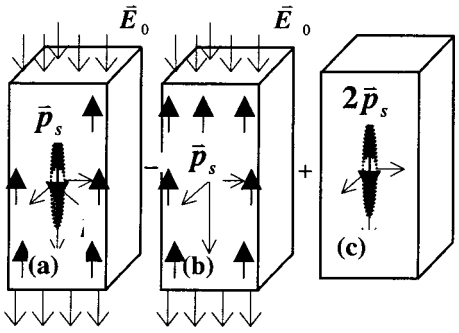

FIG. 1. A 180° domain grows in a parent phase driven by an electric field.

Consider a ferroelectric crystal below its Curie temperature. The dependence of the polarization of the crystal on the applied electric field is sketched in Fig. 2. The crystal exhibits permanent polarization $\vec{P}_S$ even in the absence of external electric fields. The parameter $\vec{P}_S$ is also called the spontaneous polarization. The constitutive equation for the ferroelectric crystal can be expressed in the following form:

$$\vec{D}=\tilde{\epsilon}\cdot\vec{E}+\vec{P}_S, \tag{1}$$

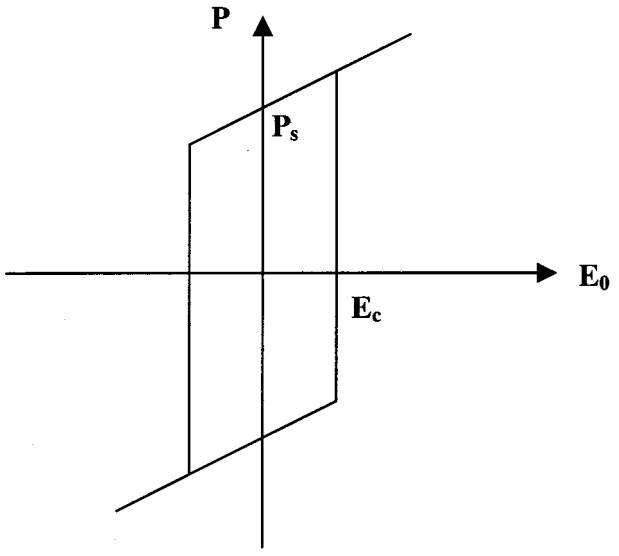

FIG. 2. Schematic of dependence $P(E)$ on the applied electric field E_0 for a ferroelectric crystal, where P_s is the spontaneous polarization and E_c is the coercive field.

where $\tilde{\epsilon}$ is the dielectric permittivity tensor, $\vec{D}$ is the electric induction, and $\vec{E}$ is the total electric field. The ferroelectric crystals can be made to be equivalent to an ordinary dielectric material with a uniform distribution of spontaneous polarization. If we apply a high enough electric field opposite to the spontaneous polarization of the ferroelectric crystal, the spontaneous polarization in some regions will begin to reverse its direction. Such regions are called the 180° domain. Those 180° domains will grow until all the spontaneous dipole moments in the crystal switch off their direction. In the current investigation, the 180° growing domain is modeled as an ellipsoid. In this section the electric field and magnetic field around it is derived. Based on the solution, an energy criterion for the domain growing will be established.

A. The electric and magnetic field of subproblem 1 [Fig. 1(b)]

As we discussed before, the ferroelectric crystal can be treated as an ordinary dielectric material with spontaneous polarization $\vec{P}_s$. The uniform polarization will generate a charge distribution on the surface of the crystal, which creates a macroscopic electric field $-\vec{P}_s/\epsilon$. If the applied electric field in the dielectric material without the spontaneous polarization is $\vec{e}_0$, the total electric and magnetic field in the crystal is given by

$$\vec{E}_0=\vec{e}_0-\frac{\vec{P}_s}{\epsilon}, \quad \vec{H}=0, \tag{2}$$

where $\vec{E}_0$ is usually treated as the applied electric field in the ferroelectric crystal when we study the domain reverse problem.

B. The electric and magnetic field of subproblem 2 [Fig. 1(c)]

The subproblem 2 is that, in an ordinary dielectric material, there is a growing, 180° domain with the spontaneous polarization $2\vec{P}_s$. This is an electrodynamic problem. If the 180° domain is assumed to take an ellipsoidal shape with principle half axes a_1, a_2, a_3, using the full Maxwell's equation, one can obtain the Hertz potential $\vec{\Pi}$ as follows:

$$\vec{\Pi}=\frac{p_s\vec{k}}{2\pi\epsilon}\int\int\int_{\Omega(t)} dv'\frac{1}{|\vec{r}-\vec{r}'|}$$

$$=\frac{p_s\vec{k}}{4\pi\epsilon}[I(\lambda)-x_n x_n I_N(\lambda)], \tag{3}$$

where $x_n x_n I_N(\lambda)=x_1^2 I_1(\lambda)+x_2^2 I_2(\lambda)+x_3^2 I_3(\lambda)$, and the expressions of λ, I, I_1, I_2, I_3, together with the detailed derivation of Eq. (3) are given in the Appendix.

By using the Hertz potential given in Eq. (3), the electric and magnetic field can be derived as follows:

$$E_1=\frac{\partial^2\Pi_3}{\partial x_1\partial x_3},$$

$$E_2=\frac{\partial^2\Pi_3}{\partial x_2\partial x_3}, \tag{4}$$

$$E_3=\frac{\partial^2\Pi_3}{\partial x_3^2}-\frac{1}{c^2}\frac{\partial^2\Pi_3}{\partial t^2}\approx\frac{\partial^2\Pi_3}{\partial x_3^2},$$

and the magnetic field $\vec{H}$ is obtained as

$$\vec{H}=\frac{1}{\xi c}\left[\frac{\partial}{\partial x_2}\left(\frac{\partial\Pi_3}{\partial t}\right)\vec{i}-\frac{\partial}{\partial x_1}\left(\frac{\partial\Pi_3}{\partial t}\right)\vec{j}\right], \tag{5}$$

where $\xi=\sqrt{\mu/\epsilon}$, $c=1/\sqrt{\epsilon\mu}$, ϵ, μ are the permittivity and permeability of the crystal, respectively, and c is the light speed in the crystal.

C. The electric and magnetic field inside the 180° domain for the original problem [Fig. 1(a)]

For interior points of an ellipsoid $\Omega(t)$, $\lambda=0$, therefore, I, I_i become constants. Substituting Eq. (3) into Eq. (4), then taking the sum of Eq. (2) and Eq. (4), one obtains the electric field inside the domain as follows:

$$E_1^{\text{in}}=0,$$

$$E_2^{\text{in}}=0, \tag{6}$$

$$E_3^{\text{in}}=E_0-\frac{p_s}{2\pi\epsilon}I_3.$$

With the aid of Eq. (5), we have

$$\vec{H}^{\text{in}}=\frac{p_s}{2\pi}\left(x_1\frac{\partial I_1}{\partial t}\vec{j}-x_2\frac{\partial I_2}{\partial t}\vec{i}\right). \tag{7}$$

It is worth mentioning that for an ellipsoidal domain, the electric field remains uniform within the domain for uniform polarization. This conclusion is similar to that obtained by Eshelby[16] for elastic problems. For spherical domain with radius a

$$I=4\pi a^2, \quad I_1=I_2=I_3=\tfrac{4}{3}\pi. \tag{8}$$

Substitution of Eq. (8) into Eqs. (6) and (7) yields

$$E_3^{\text{in}}=E_0-\frac{2p_s}{3\epsilon},$$

$$\vec{H}^{\text{in}}=0. \tag{9}$$

The other components of the electric field within the domain are zero.

D. The electric and magnetic field outside the 180° domain for the original problem [Fig. 1(a)]

By substituting Eq. (3) into Eq. (4) and adding Eq. (2), we obtain the electric field outside the domain as

$$E_1^{\text{out}}=\frac{\partial^2\Pi_3}{\partial x_1\partial x_3}=\frac{p_s}{4\pi\epsilon}\frac{\partial^2}{\partial x_1\partial x_3}[I(\lambda)-x_n x_n I_N(\lambda)],$$

$$E_2^{\text{out}}=\frac{\partial^2\Pi_3}{\partial x_2\partial x_3}=\frac{p_s}{4\pi\epsilon}\frac{\partial^2}{\partial x_2\partial x_3}[I(\lambda)-x_n x_n I_N(\lambda)], \tag{10}$$

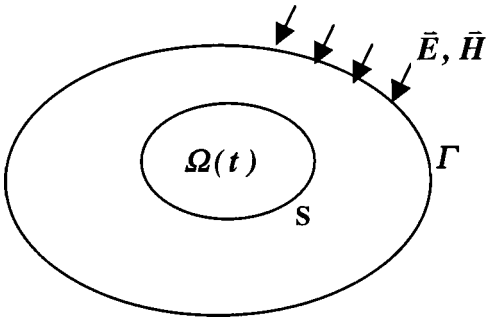

FIG. 3. A surface of discontinuity in an electromagnetic field.

$$E_3^{\text{out}} = E_0 - \left(\frac{1}{c^2}\frac{\partial^2 \Pi_3}{\partial t^2} - \frac{\partial^2 \Pi_3}{\partial x_3^2}\right) = E_0 - \frac{p_s}{4\pi\epsilon}\left(\frac{1}{c^2}\frac{\partial^2}{\partial t^2} - \frac{\partial^2}{\partial x_3^2}\right)[I(\lambda) - x_n x_n I_N(\lambda)],$$

where the magnetic field is given by Eq. (5)

$$\vec{H}^{\text{out}} = \frac{1}{\xi c}\left[\frac{\partial}{\partial x_2}\left(\frac{\partial \Pi_3}{\partial t}\right)\vec{i} - \frac{\partial}{\partial x_1}\left(\frac{\partial \Pi_3}{\partial t}\right)\vec{j}\right] = \frac{p_s}{4\pi}\left(\frac{\partial}{\partial x_2}\vec{i} - \frac{\partial}{\partial x_1}\vec{j}\right)\frac{\partial}{\partial t}[I(\lambda) - x_n x_n I_N(\lambda)]. \quad (11)$$

In deriving Eq. (11), we have used $c^2 = 1/\epsilon\mu$, and $\xi = \sqrt{\mu/\epsilon}$.

III. ENERGY CONCEPT AND THE DRIVING FORCE FOR THE 180° DOMAIN EXPANDING

Starting with a general case, we consider a general shape of the 180° domain wall in an electromagnetic field (Fig. 3). The surface can move under the action of the electric and magnetic field. With the movement of the surface, the electromagnetic energy will be reduced, and the released energy serves as the driving force to compensate the energy dissipation in the moving process of the surface. The energy dissipation is due to the surface energy increase and the finite velocity of the movement. In this part, a general form of the energy release rate will be derived. As an application, the energy release rate will be used to establish an equation to determine the growth rate of the 180° domain wall. In fact, the obtained expression to calculate the energy release rate is suitable for the movement of any surface of discontinuity in an electromagnetic field. Here a surface of discontinuity means that some components of the electric and magnetic field may have certain jump due to physical mechanism across the surface. The 180° domain wall is only an example of such surfaces.

As shown in Fig. 3, the body containing a surface of discontinuity in an electromagnetic field can be divided into two regions, i.e., inside and outside the surface. The internal energy of an electromagnetic field is given by

$$W = \frac{1}{2}\int_v \int\int (\vec{E}\vec{D} + \vec{H}\vec{B})dv = \int_{\Omega(t)} \int\int \Phi dv + \int_{v-\Omega(t)} \int\int \Phi dv = W_1 + W_2, \quad (12)$$

where $\Omega(t)$, v are the volumes inside the moving surface and the whole body, respectively. $\Phi = 1/2(\vec{E}\vec{D} + \vec{H}\vec{B})$ is the energy density. In the following we need to derive the change rate of the energy. For the first integral in Eq. (12), the region of integration and the integrand are the function of time t. Using Reynolds' transport theorem,[27] its change rate is obtained as:

$$\frac{dW_1}{dt} = \frac{d}{dt}\int_{\Omega(t)} \int\int \Phi dv = \int_{\Omega(t)} \int\int [\dot{\Phi} + \text{div}(\Phi \vec{u})]dv = \int_{\Omega(t)} \int\int \dot{\Phi} dv + \int_{s^+} \int\int \Phi \vec{u}\cdot\vec{n} ds, \quad (13)$$

where $\vec{u}$ is the velocity of the surface movement and S^+ is the internal side of the surface. Equation (13) asserts that the changing rate of the integral Φ over $\Omega(t)$ is equal to the rate computed as if $\Omega(t)$ were fixed in its current position plus the rate at which Φ is carried out of this region across its boundary. The rate of the energy density is given by

$$\dot{\Phi} = \frac{1}{2}\frac{d}{dt}(\vec{E}\vec{D} + \vec{H}\vec{B}) = \vec{E}\dot{\vec{D}} + \vec{H}\dot{\vec{B}} = \vec{E}\cdot(\nabla\times\vec{H} - \vec{J}) + \vec{H}\cdot(-\nabla\times\vec{E}) = -\vec{E}\vec{J} - [\vec{H}\cdot(\nabla\times\vec{E}) - \vec{E}\cdot(\nabla\times\vec{H})] = -\vec{E}\vec{J} - \text{div}(\vec{E}\times\vec{H}). \quad (14)$$

In deriving Eq. (14), we have used Maxwell's equation to replace the time-derivative factors in the integrand, $\vec{\Sigma} = \vec{E}\times\vec{H}$, where $\vec{\Sigma}$ is called the Poynting vector, which is identified as the energy flux, or rate of energy flow per unit area. Substitution of Eq. (14) into Eq. (13), and considering the current $\vec{J} = 0$ inside the region, we have

$$\frac{dW_1}{dt} = \int_{S^+} \int\int [\Phi\vec{u} - \vec{\Sigma}]\cdot\vec{n} ds. \quad (15)$$

In a similar way, one can derive the rate of the second integral in Eq. (12) as follows:

$$\frac{dW_2}{dt} = -\int_{\Gamma} \int\int \vec{\Sigma}\cdot\vec{n} ds + \int_{S^-} \int\int [\vec{\Sigma} - \Phi\vec{u}]\cdot\vec{n} ds, \quad (16)$$

where S^- is the external side of the surface and Γ is the outside boundary of the body. The changing rate of the energy provided by the environment across the outside boundary of the body is given by

$$\dot{U} = -\int_{\Gamma}\int \vec{\Sigma}\cdot\vec{n}ds. \tag{17}$$

Therefore the energy release rate in the process of surface movement can be obtained as

$$\dot{G} = \dot{U} - \dot{W} = \int_{S}\int \{[\Phi]u_i - [\Sigma_i]\}n_i ds, \tag{18}$$

where $[\Phi] = \Phi^0 - \Phi^I$, $[\Sigma_i] = \Sigma_i^0 - \Sigma_i^I$ are the jumps of corresponding quantities across the surface. Eshelby[17] proposed the well-known energy–momentum tensor as the driving force for a defect to propagate in materials. In fact, Eq. (18) represents its counterpart in an electromagnetic field. Similarly, we can define the energy–momentum vector as[18–21]

$$P_i = \Phi u_i - \Sigma_i. \tag{19}$$

The energy release rate $\dot{G}$ represents the driving force for the growth of the 180° domain. For a general domain wall movement problem, one can develop an efficient numerical method to evaluate the surface integral. In what follows, we use Eq. (18) to calculate the energy release rate for the growth of the spherical and cylindrical domains.

IV. A SPHERICAL 180° DOMAIN EXAMPLE AND DISCUSSION

In this section, we consider the spherical 180° domain as an example to derive the explicit close-form solution of the energy release rate. The spherical domain can be used to model the nuclei of the 180° domain. In this part of the article, we consider that the spherical nuclei grow up along the radial direction and along the direction of the applied field, respectively.

A. The spherical domain grows along the radial direction

In such a case, the spherical domain will remain its spherical shape in the propagation process. Therefore the internal electric field is given by

$$E_1^I = E_2^I = 0, \quad E_3^I = E_0 - \frac{2}{3}\cdot\frac{p_s}{\epsilon} \tag{20}$$

and the internal magnetic field remains zero. The electric field outside the domain is given by Eq. (10) as follows:

$$\begin{aligned} E_1^0 &= \frac{2p_s}{\epsilon}\cdot\left(\frac{a}{r}\right)^3 \sin\theta\cos\theta\cos\varphi, \\ E_2^0 &= \frac{2p_s}{\epsilon}\cdot\left(\frac{a}{r}\right)^3 \sin\theta\cos\theta\sin\varphi, \\ E_3^0 &= E_0 - \frac{2}{3}\frac{p_s}{\epsilon}\cdot\left(\frac{a}{r}\right)^3 + \frac{2p_s}{\epsilon}\cdot\left(\frac{a}{r}\right)^3 \cos^2\theta. \end{aligned} \tag{21}$$

The magnetic field is obtained from Eq. (11)

$$\vec{H}^0 = 2p_s\left(\frac{a}{r}\right)^2\frac{da}{dt}(\sin\theta\cos\varphi\vec{j} - \sin\theta\sin\varphi\vec{i}). \tag{22}$$

Substituting the expressions of the electric field and magnetic field into Eq. (18), one can derive the energy release rate after the integration

$$\dot{G} = \frac{8\pi a^2}{3}\cdot\frac{da}{dt}\left[3p_sE_0 - \frac{p_s^2}{\epsilon} + 2\mu p_s^2\left(\frac{da}{dt}\right)^2\right]. \tag{23}$$

The energy release rate can also be expressed in the form of

$$\dot{G} = g\cdot\frac{da}{dt}, \tag{24}$$

where $g = \partial G/\partial a$ is the energy reduction per unit increase of the domain radius. If the surface energy density of the 180° domain wall is denoted as U_s, the surface energy will increase $8\pi a U_s$ per unit increase of the domain radius. Domain evolution is a nonequilibrium thermodynamics process, and its evolution velocity can be reasonably assumed to be proportional to the total free energy reduction[4] as follows:

$$\begin{aligned} \frac{da}{dt} &= M(g - 8\pi a U_s) \\ &= M\left\{\frac{8\pi a^2}{3}\cdot\left[3p_sE_0 - \frac{p_s^2}{\epsilon} + 2\mu p_s^2\left(\frac{da}{dt}\right)^2\right] - 8\pi a U_s\right\}. \end{aligned} \tag{25}$$

If the initial velocity is zero, one can obtain the critical electric field for the domain to grow along the radial direction through the following equation:

$$ap_sE_0 - \frac{ap_s^2}{3\epsilon} - U_s = 0. \tag{26}$$

As a numerical example, considering the typical ferroelectric material barium titanete $BaTiO_3$, the material constants are as follow:[4,25]

$$p_s = 0.26\ \text{C/m}^2, \quad \epsilon = 1.8\times10^{-8}\ \text{F/m},$$

$$U_s = 0.01\ \text{J/m}^2, \quad a = 1\ \mu\text{m}.$$

By substitutiing these values into Eq. (26), one obtains the critical electric field

$$E_0 \approx 4.8\ \text{MV/m}. \tag{27}$$

The critical field for the radial movement of the domain wall is so high that it is almost impossible in practice.

B. The spherical domain grows along the direction of the applied field

It is a widely accepted phenomenon that the 180° domain wall will prefer to move along the direction of the applied field when a single-domain crystal is placed into an electric field opposite the polar direction. In this part, we will derive the energy release rate when a spherical domain starts to grow along the direction of the applied field. Since the domain will not keep its spherical shape once it starts to grow in this case, we should consider a general spheroid shape of the domain to derive the solution of electric and

magnetic fields. To obtain the energy release rate from Eq. (18), we need to know the electric and magnetic field inside the domain and just outside the domain. According to Eqs. (6) and (7), the electric and magnetic field inside the domain are given by

$$E_1^I = E_2^I = 0, \quad E_3^I = E_0 - \frac{2p_s}{3\epsilon},$$
$$\vec{H}^I = \frac{4p_s}{15a}(x_1\vec{j} - x_2\vec{i})\frac{da_3}{dt}, \tag{28}$$

where da_3/dt represents the velocity of the semiaxis change of the domain along the z direction. The field just outside the domain can be obtained through the continuity condition across the surface given by

$$\vec{n}\times(\vec{E}^0 - \vec{E}^I) = 0, \quad \epsilon\vec{n}\cdot(\vec{E}^0 - \vec{E}^I) = 2p_s\vec{k}\cdot\vec{n},$$
$$\vec{n}\cdot(\vec{H}^0 - \vec{H}^I) = 0, \quad \vec{n}\times(\vec{H}^0 - \vec{H}^I) = 2p_s\dot{R}(t)[\vec{k} - (\vec{n}\cdot\vec{k})\vec{n}], \tag{29}$$

where $\vec{n}$, $\vec{R}(t)$ are the outward normal vector, and the change rate of the point's distance from the origin on the wall. The electric and magnetic field just outside the domain are thus obtained from Eq. (29) as

$$\vec{E}^0 = \vec{E}^I + \frac{2p_s}{\epsilon}(\vec{k}\cdot\vec{n})\vec{n},$$
$$\vec{H}^0 = \vec{H}^I + 2p_s\dot{R}(t)\vec{k}\times\vec{n}. \tag{30}$$

Substitution of Eqs. (28) and (30) into Eq. (18) gives the energy release rate

$$\dot{G} = \frac{8\pi a^2}{3}\cdot\frac{da_3}{dt}\left[p_sE_0 - \frac{p_s^2}{15\epsilon} + 0.2362\mu p_s^2\left(\frac{da_3}{dt}\right)^2\right]. \tag{31}$$

As in the last part, if the initial velocity is zero, one can obtain the critical electric field for the domain to grow along the direction of the applied electric field through the following equation:

$$ap_sE_0 - \frac{ap_s^2}{15\epsilon} - U_s = 0. \tag{32}$$

For $BaTiO_3$, one can calculate the critical electric field as

$$E_0 = 0.97 \ \text{MV/m}. \tag{33}$$

Comparing with Eq. (27), we can find that the critical electric field for such movement is only one fifth of the value for the radial movement. This may explain why the 180° domain always grows along the direction of the applied electric field.

V. A CYLINDRICAL 180° DOMAIN EXAMPLE

When a single-domain crystal is placed into an electric field opposite to the polar direction, numerous 180° domain spikes emerge.[4,26] They grow much faster in the direction of the applied field than in the normal direction. The forward velocity was found experimentally to vary with the applied electric field as[26]

$$\frac{dL}{dt} = M_0(E - E_c), \tag{34}$$

where M_0 and E_c are the parameters to fit the experimental data for $BaTiO_3$, $M_0 = 2.5\times10^{-4}\ \text{m}^2/\text{V s}$, and $E_c = 0.22$ MV/m at room temperature. This experimental result can be interpreted according to the energy model.

A spike can be modeled as a long cylindrical domain with the length L and radius a. The electric and magnetic field inside the domain and just outside the domain can be obtained by using Eqs. (6), (7), and (30) under the condition $L \gg a$. By substituting them into Eq. (18), we obtain the energy release rate as

$$\dot{G} = 2\pi a^2E_0p_s\dot{L}. \tag{35}$$

The energy reduction due to the unit increase of the length L is given by

$$g = 2\pi a^2E_0p_s. \tag{36}$$

In the same way as deriving Eq. (25), one can obtain the velocity equation as

$$\frac{dL}{dt} = M(g - 2\pi aU_s) = 2\pi a^2Mp_s\left(E_0 - \frac{U_s}{ap_s}\right). \tag{37}$$

By comparing the experiment result with Eq. (34), one can obtain an estimate of the domain wall energy U_s

$$U_s = ap_sE_c. \tag{38}$$

Taking the experimental values $a = 0.5\ \mu$m, $p_s = 0.26\ \text{C/m}^2$, and $E_c = 0.22$ MV/m, we find that $U_s = 0.0286\ \text{J/m}^2$. This estimate is just within the range of experimental data for $BaTiO_3$.[25]

ACKNOWLEDGMENT

This work was partly supported by The National Natural Science Foundation of China through the Fund for Excellent Young Investigators.

APPENDIX: DERIVATION OF THE ELECTRIC AND MAGNETIC FIELD FOR A GROWING, 180° DOMAIN

In any time-invariant reference system of coordinates, the differential form of Maxwell's equations reads as follows:[13]

$$\nabla\times\vec{E} = -\frac{\partial\vec{B}}{\partial t}, \tag{A1a}$$
$$\nabla\times\vec{H} = \vec{J} + \frac{\partial\vec{D}}{\partial t}, \tag{A1b}$$
$$\nabla\cdot\vec{D} = \rho, \tag{A1c}$$
$$\nabla\cdot\vec{B} = 0, \tag{A1d}$$

where $\vec{E}$ is electric field (V/m); $\vec{H}$ is magnetic field (A/m); $\vec{D}$ is electric induction (C/m^2); $\vec{B}$ is magnetic induction (T); $\vec{J}$ is electric current density (A/m^2); and ρ is electric charge density (C/m^2), and the prescribed source current $\vec{J}$ and charge density ρ are related by the continuity equation

$$\nabla \cdot \vec{J} + \frac{\partial \rho}{\partial t} = 0. \tag{A2}$$

In the present work, we impose a further simplification by ignoring the anisotropic effect of the dielectric constant. For linear isotropic materials, the constitutive relation can be written as follows:

$$\begin{aligned} \vec{D} &= \epsilon \vec{E}, \\ \vec{B} &= \mu \vec{H}, \end{aligned} \tag{A3}$$

where ϵ, μ are the permittivity and permeability of the isotropic medium, respectively.

The electric polarization gives rise to the charge distribution with volume density[14]

$$\rho = -\nabla \cdot (2\vec{P}_s). \tag{A4a}$$

If the polarization changes with time, similarly, it corresponds to the current density as follows:

$$\vec{J} = \frac{\partial (2\vec{P}_s)}{\partial t}. \tag{A4b}$$

By taking the curl of Eq. (A1a) and substituting $\nabla \times \vec{H}$ from Eq. (A1b), we obtain

$$\nabla \times \nabla \times \vec{E} = -\mu \epsilon \frac{\partial^2 \vec{E}}{\partial t^2} - \mu \frac{\partial \vec{J}}{\partial t}. \tag{A5}$$

Combination of Eqs. (A1c) and (A5) yields

$$\nabla^2 \vec{E} - \frac{1}{c^2} \frac{\partial^2 \vec{E}}{\partial t^2} = \mu \frac{\partial \vec{J}}{\partial t} + \frac{1}{\epsilon} \nabla \rho, c^2 = 1/\epsilon\mu. \tag{A6a}$$

Substitution of Eq. (A4) into Eq. (A6a) leads to

$$\nabla^2 \vec{E} - \frac{1}{c^2} \frac{\partial^2 \vec{E}}{\partial t^2} = \left(\frac{1}{c^2} \frac{\partial^2}{\partial t^2} I - \nabla \nabla \right) \cdot \frac{2\vec{P}_s}{\epsilon}, \tag{A6b}$$

where I is the diagonal unit matrix. The above equation relates the unknown electric field with the source field $2\vec{P}_s/\epsilon$. By introducing the Hertz potential $\vec{\Pi}$ as follows:

$$\begin{bmatrix} E_1 \\ E_2 \\ E_3 \end{bmatrix} = - \begin{bmatrix} \frac{1}{c^2}\frac{\partial^2}{\partial t^2} - \frac{\partial^2}{\partial x^2} & -\frac{\partial^2}{\partial x \partial y} & -\frac{\partial^2}{\partial x \partial z} \\ -\frac{\partial^2}{\partial x \partial y} & \frac{1}{c^2}\frac{\partial^2}{\partial t^2} - \frac{\partial^2}{\partial y^2} & -\frac{\partial^2}{\partial y \partial z} \\ -\frac{\partial^2}{\partial x \partial z} & -\frac{\partial^2}{\partial y \partial z} & \frac{1}{c^2}\frac{\partial^2}{\partial t^2} - \frac{\partial^2}{\partial z^2} \end{bmatrix} \times \begin{bmatrix} \Pi_1 \\ \Pi_2 \\ \Pi_3 \end{bmatrix}, \tag{A7}$$

we have

$$\nabla^2 \vec{\Pi} - \frac{1}{c^2} \frac{\partial^2 \vec{\Pi}}{\partial t^2} = -\frac{2\vec{P}_s}{\epsilon}. \tag{A8}$$

Once the Hertz potential $\vec{\Pi}$ is determined, the electric field can be found through Eq. (A7), while the magnetic field is computed from Eq. (A1a):

$$\xi \vec{H} = \nabla \times \frac{1}{c} \frac{\partial \vec{\Pi}}{\partial t}, \quad \xi = \sqrt{\mu/\epsilon}. \tag{A9}$$

For such a problem, we first need to derive the solution for the following equation subjected to the initial condition $G(\vec{r}, t<0) = 0$ and to the radiation conditions at infinity as the Green's function:

$$\nabla^2 G(\vec{r}, t) - \frac{1}{c^2} \frac{\partial^2 G(\vec{r}, t)}{\partial t^2} = -\delta(\vec{r})\delta(t). \tag{A10}$$

The solution of Eq. (A10) in a spherical system of coordinates is

$$G(\vec{r}, t) = \frac{\delta(t - r/c)}{4\pi r} = \frac{\delta(t^*)}{4\pi r}, \tag{A11}$$

where $t^* = t - r/c$ is the retarded time, $\vec{r}$ is the position vector, and r is its magnitude.

Green's function represents the response of the system described by Eq. (A10) to a localized unit source of space–time density $\delta(\vec{r})\delta(t)$. It can be used to derive the final expression for the field radiated by an arbitrary source distribution. For the present case, the applied source is the dipole density $2\vec{P}(\vec{r}, t)/\epsilon$. The total Hertz potential can be obtained by superposition as shown in Eqs. (A8) and (A10):

$$\begin{aligned} \vec{\Pi} &= 2 \int\int\int dv' \int dt' \frac{\vec{P}_s(\vec{r}', t')}{\epsilon} G(\vec{r} - \vec{r}', t - t') \\ &= \frac{1}{2\pi\epsilon} \int\int\int dv' \int dt' \vec{P}_s(\vec{r}', t') \\ &\quad \times \frac{\delta(t - t' - |\vec{r} - \vec{r}'|/c)}{|\vec{r} - \vec{r}'|} \\ &= \frac{1}{2\pi\epsilon} \int\int\int dv' \frac{\vec{P}_s(\vec{r}', t^*)}{|\vec{r} - \vec{r}'|}, \end{aligned} \tag{A12}$$

where $t^* = t - |\vec{r} - \vec{r}'|/c$. For the current problem, the polarization source is restricted to the finite region. Generally speaking, since c is the light speed, $ct \gg |\vec{r} - \vec{r}|$. Therefore the polarization can be expressed using the Heaviside function as follows:

$$\vec{P}_s(\vec{r}, t^*) \approx \vec{P}_s(\vec{r}, t) = p_s \vec{k} H[\Omega(t)], \tag{A13}$$

where

$$H[\Omega(t)] = \begin{cases} 1 & \vec{r} \in \Omega(t) \\ 0 & \text{others} \end{cases}, \tag{A14}$$

in which $\Omega(t)$ is the region of 180° domain. Since the domain is expanding, it is a function of time. In what follows, we assume that the 180° domain takes an ellipsoidal shape, and derive the electric and magnetic field both inside and outside the domain.

Substitution of Eq. (A13) into Eq. (A12) yields

$$\vec{\Pi} = \frac{p_s \vec{k}}{2\pi\epsilon} \int_{\Omega(t)} \int\int dv' \frac{1}{|\vec{r} - \vec{r}'|}. \tag{A15}$$

If the 180° domain is assumed to take an ellipsoidal shape with principle half axes a_1, a_2, a_3, the integral in Eq. (A15) can be expressed in terms of the following simple formula as shown in Mura:[15]

$$\vec{\Pi}=\frac{p_s\vec{k}}{2\pi\epsilon}\int\int_{\Omega(t)}\int dv'\frac{1}{|\vec{r}-\vec{r}'|}=\frac{p_s\vec{k}}{4\pi\epsilon}[I(\lambda)-x_nx_nI_N(\lambda)], \tag{A16}$$

where $x_nx_nI_N(\lambda)=x_1^2I_1(\lambda)+x_2^2I_2(\lambda)+x_3^2I_3(\lambda)$, and the expressions of λ, I, I_1, I_2, I_3 are given as follows:

$$\begin{aligned}I(\lambda)&=2\pi a_1a_2a_3\int_\lambda^\infty\frac{ds}{\Delta(s)},\\ I_i(\lambda)&=2\pi a_1a_2a_3\int_\lambda^\infty\frac{ds}{(a_i^2+s)\Delta(s)},\end{aligned} \tag{A17}$$

where $\Delta(s)=[(a_1^2+s)(a_2^2+s)(a_3^2+s)]^{1/2}$, and λ is the largest positive root of the equation

$$\frac{x_1^2}{(a_1^2+\lambda)}+\frac{x_2^2}{(a_2^2+\lambda)}+\frac{x_3^2}{(a_3^2+\lambda)}=1. \tag{A18}$$

Thus

$$\begin{aligned}I(\lambda)&=4\pi a_1a_2a_3(a_1^2-a_3^2)^{-1/2}F(\theta,k),\\ I_1(\lambda)&=4\pi a_1a_2a_3(a_1^2-a_2^2)^{-1}(a_1^2-a_3^2)^{-1/2}\\ &\quad\times[F(\theta,k)-E(\theta,k)],\\ I_2(\lambda)&=4\pi a_1a_2a_3[(a_1^2-a_3^2)^{1/2}(a_1^2-a_2^2)^{-1}\\ &\quad\times(a_2^2-a_3^2)^{-1}E(\theta,k)-(a_1^2-a_2^2)^{-1}\\ &\quad\times(a_1^2-a_3^2)^{-1/2}F(\theta,k)-(a_2^2-a_3^2)^{-1}\\ &\quad\times(a_3^2+\lambda)^{1/2}(a_1^2+\lambda)^{-1/2}(a_2^2+\lambda)^{-1/2}],\\ I_3(\lambda)&=4\pi a_1a_2a_3(a_2^2-a_3^2)^{-1}(a_1^2-a_3^2)^{-1/2}\\ &\quad\times[(a_2^2+\lambda)^{1/2}(a_1^2-a_3^2)^{1/2}(a_1^2+\lambda)^{-1/2}\\ &\quad\times(a_3^2+\lambda)^{-1/2}-E(\theta,k)],\end{aligned} \tag{A19}$$

where the first and second elliptic integrals are given by

$$\begin{aligned}F(\theta,k)&=\int_0^\theta\frac{dw}{(1-k^2\sin^2w)^{1/2}},\\ E(\theta,k)&=\int_0^\theta(1-k^2\sin^2w)^{1/2}dw,\\ \theta&=\sin^{-1}(1-a_3^2/a_1^2)^{1/2},\quad k=[(a_1^2-a_2^2)/(a_1^2-a_3^2)]^{1/2}.\end{aligned} \tag{A20}$$

For some special shapes of the domain, Eq. (A19) becomes elementary functions and are shown below.

1. Sphere ($a_1=a_2=a_3=a$)

$$\begin{aligned}I(\lambda)&=\frac{4\pi a^3}{(a^2+\lambda)^{1/2}},\\ I_1(\lambda)&=I_2(\lambda)=I_3(\lambda)=\frac{4\pi a^3}{3(a^2+\lambda)^{3/2}}.\end{aligned} \tag{A21}$$

2. Elliptical cylinder ($a_3\to\infty$)

$$\begin{aligned}I(\lambda)&=0,\\ I_1(\lambda)&=\frac{4\pi a_1a_2}{a_2^2-a_1^2}\left[\frac{(a_2^2+\lambda)^{1/2}}{(a_1^2+\lambda)^{1/2}}-1\right],\\ I_2(\lambda)&=\frac{4\pi a_1a_2}{a_1^2-a_2^2}\left[\frac{(a_1^2+\lambda)^{1/2}}{(a_2^2+\lambda)^{1/2}}-1\right],\\ I_3(\lambda)&=0.\end{aligned} \tag{A22}$$

3. Oblate spheroid ($a_1=a_2>a_3$)

$$\begin{aligned}I(\lambda)&=\frac{4\pi a_1^2a_3}{\sqrt{a_1^2-a_3^2}}\arccos b,\\ I_1(\lambda)&=I_2(\lambda)=2\pi a_1^2a_3(\arccos b-bd)/(a_1^2-a_3^2)^{3/2},\\ I_3(\lambda)&=4\pi a_1^2a_3\left(\frac{d}{b}-\arccos b\right)/(a_1^2-a_3^2)^{3/2},\end{aligned} \tag{A23}$$

where $b=\sqrt{(a_3^2+\lambda)/(a_1^2+\lambda)}$ and $d=\sqrt{(a_1^2-a_3^2)/(a_1^2+\lambda)}$.

4. Prolate spheroid ($a_1>a_2=a_3$)

$$\begin{aligned}I(\lambda)&=\frac{4\pi a_1a_3^2}{\sqrt{a_1^2-a_3^2}}\operatorname{arccos\,h}\bar{b},\\ I_1(\lambda)&=4\pi a_1a_3^2(\operatorname{arccos\,h}\bar{b}-\bar{d}/\bar{b})/(a_1^2-a_3^2)^{3/2},\\ I_2(\lambda)&=I_3(\lambda)=2\pi a_1a_3^2(\bar{b}\bar{d}-\operatorname{arccos\,h}\bar{b})/(a_1^2-a_3^2)^{3/2},\end{aligned} \tag{A24}$$

where $\bar{b}=\sqrt{(a_1^2+\lambda)/(a_3^2+\lambda)}$ and $\bar{d}=\sqrt{(a_1^2-a_3^2)/(a_3^2+\lambda)}$.

If the point is inside the domain, $\lambda=0$.

[1] R. Landauer, J. Appl. Phys. **28**, 227 (1957).
[2] J. M. Rickman, N. Sridhar, and D. J. Srolovitz, Acta Mater. **47**, 1325 (1999).
[3] J. S. Speck, A. C. Daykin, A. Seifert, A. E. Romanov, and W. Pompe, J. Appl. Phys. **78**, 1695 (1995).
[4] R. E. Loge and Z. Suo, Acta Mater. **44**, 3429 (1996).
[5] V. Gopalan and T. E. Mitchell, J. Appl. Phys. **83**, 941 (1998).
[6] Y. Huo and Q. Jiang, Smart Mater. Struct. **6**, 441 (1997).
[7] Y. Huo and Q. Jiang, Int. J. Solids Struct. **35**, 1339 (1998).
[8] P. Rosakis and Q. Jiang, Int. J. Eng. Sci. **33**, 1 (1995).
[9] S. C. Hwang, C. S. Lynch, and R. M. McMeeking, Acta Metall. Mater. **43**, 2073 (1995).
[10] W. Lu, D. N. Fang, C. Q. Li, and K. C. Hwang, Acta Mater. **47**, 2913 (1999).
[11] W. Yang and Z. Suo, J. Mech. Phys. Solids **42**, 649 (1994).
[12] J. Li and G. J. Weng, Proc. R. Soc. London, Ser. A **455**, 3493 (1999).
[13] D. R. Frankl, *Electromagnetic Theory* (Prentice-Hall, Englewoods Cliff, NJ, 1986).
[14] G. Franceschetti, *Electromagnetics: Theory, Technique, and Engineering Paradigms* (Plenum, New York, 1997).
[15] T. Mura, *Micromechanics of Defects in Solids*, 2nd rev. ed. (Martinus Nijhoff, Dordrecht, 1987).
[16] J. D. Eshelby, Proc. R. Soc. London, Ser. A **241**, 376 (1957).
[17] J. D. Eshelby, *Inelastic Behavior of Solids* (McGraw-Hill, New York, 1970).
[18] L. B. Freund, *Dynamic Fracture Mechanics* (Cambridge University Press, Cambridge, UK, 1990).
[19] B. A. Strukov and A. P. Levanyuk, *Ferroelectric Phenomena in Crystals* (Springer, Berlin, 1998).
[20] B. Wang, Int. J. Solids Struct. **29**, 293 (1992).

[21] B. Wang, Acta Mater. **45**, 1551 (1997).
[22] C. S. Lynch and R. M. McMeeking, Ferroelectrics **160**, 177 (1994).
[23] T. J. Yang, V. Gopalan, P. J. Swart, and U. Mohideen, Phys. Rev. Lett. **82**, 4106 (1999).
[24] F. K. Chai, J. R. Brews, R. D. Schrimpf, and D. P. Birnie III, J. Appl. Phys. **82**, 2505 (1997).
[25] W. Zhong, *Physics of Ferroelectrics* (Science Sinica, 1998) (in Chinese).
[26] W. J. Mertz, Phys. Rev. **95**, 690 (1954).
[27] M. E. Gurtin, *An Introduction to Continuum Mechanics* (Academic, New York, 1981).